http://www.geojournals.cn/dzxbcn/ch/index.aspx

Geochemistry of Mesoproterozoic Volcanic Rocks in the Western Kunlun Mountains: Evidence for Plate Tectonic Evolution

ZHANG Chuanlin[1,2], DONG Yongguan[2], ZHAO Yu[2], WANG Aiguo[2] and GUO Kunyi[2]

1 *Guiyang Institute of Geochemistry, Chinese Academy of Sciences, Guiyang, Guizhou 550002; E-mail: zchuanlin@sina.com*

2 *Nanjing Institute of Geology and Mineral Resources, Nanjing, Jiangsu 210016*

Abstract Mesoproterozoic volcanic rocks occurring in the north of the western Kunlun Mountains can be divided into two groups. The first group (north belt) is an reversely-evolved bimodal series. Petrochemistry shows that the alkalinity of the rocks decreases from early to late: alkaline→calc-alkaline→tholeiite, and geochemistry proves that the volcanic rocks were formed in rifting tectonic systems. The sedimentary facies shows characteristics of back-arc basins. The second (south belt) group, which occurs to the south of Yutian-Minfeng-Cele, is composed of calc-alkaline island arc (basaltic) andesite and minor rhyolite. The space distribution, age and geochemistry of the two volcanite groups indicate that they were formed in a back-arc basin (the first group) and an island arc (the second group) respectively and indicate the plate evolution during the Mesoproterozoic. The orogeny took place at ~1.05 Ga, which was coeval with the Grenville orogeny. This study has provided important geological data for exploring the position of the Paleo-Tarim plate in the Rodinia super-continent.

Key words: western Kunlun, Mesoproterozoic volcanic rocks, geochemistry, Grenville orogeny

1 Introduction

In the north belt of the western Kunlun Mountains, along the north edge of the Kungaishan-Ke'erhan-Buqiong-Aidewagao area, there occurs the Ailiankate Group (AG for short, Fig. 1) of the Mesoproterozoic Jixianian Period (1400–1000 Ma). According to predecessors (e.g. Xinjiang Bureau of Geology and Mineral Resources, 1993), the AG is a set of metamorphic volcanic-sedimentary rocks. The lower part of it is composed of very thick metamorphic alkaline–calc-alkaline bimodal volcanic rocks, while the upper part consists of flysch and molasse, which indicate the whole course of the forming, developing and closing of a sedimentary basin. The Taxidaban Group of the Mesoproterozoic Jixianian Period (TG for short, Fig. 1), which occurs to the south of Yutian and Minfeng, is a set of low-grade metamorphic basaltic andesite and andesite

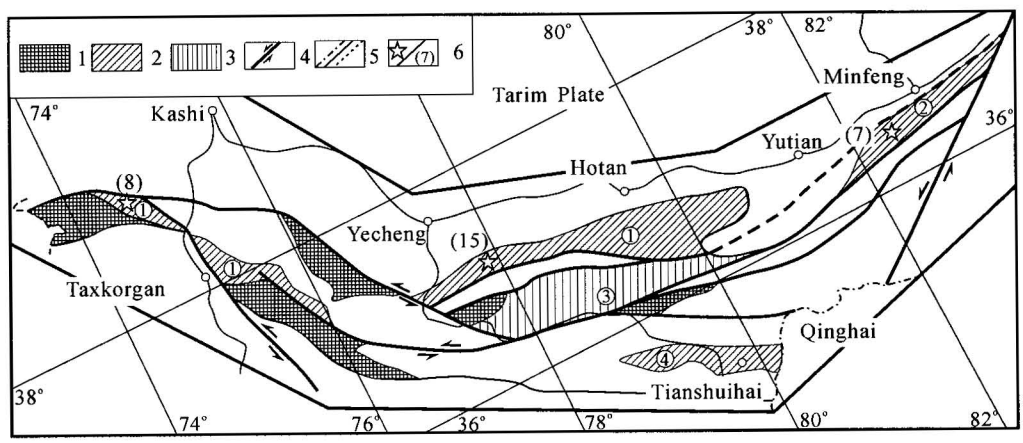

Fig. 1. Sketch map of the Precambrian of the Western Kunlun Mountains.

1. Early Precambrian high-grade metamorphic basement; 2. Mesoproterozoic volcanic-sedimentary rocks; 3. Mesoproterozoic volcanic-sedimentary sequence; 4. fault; 5. national / provincial boundaries; 6. sampling site and number of samples; ① AG of the Jixianian Period (back-arc), ② TG of the Jixianian Period (island arc), ③ Alamasi Group of the Jixianian Period (passive continental margin sedimentation), ④ Tianshuihai Group of the Changchengian Period

in addition to a small amount of rhyolite. The two sets of volcanic-sedimentary rocks comprise the main body of the Mesoproterozoic strata in the north of the western Kunlun Mountains. The Alamasi Group of the Jixianian Period, which lies in a remote mountainous region and has been poorly studied, is composed of clastic rocks (Miao, 1993). Few previous studies have touch upon the Pre-Sinian in the western Kunlun Mountains (Xiao et al., 1998; Pan, 1994; Liu et al, 1998). Stratigraphic and geochemical studies conducted for the first time on these two sets of volcanic-sedimentary rocks by the authors shows that they are the result of evolution of the southern Tarim plate during the Mesoproterozoic. The plate subduction and collision took place at ca. 1.05 Ga, which is well consistent with the Grenville orogeny. The study provides very important geological data for exploring the location of the Tarim plate in the Rodinia super-continent.

2 Geochemistry of Back-arc Basin Volcanic Rocks

This volcanic sequence, represented by the AG, mainly occurs in the Tiekelike tectonic belt in the southern Tarim plate (Fig. 1). Its sedimentary sequence represents the forming, developing and closing course of a back-arc basin (Guo et al., 2002). As the metamorphic strata have clear bedding and no alteration, geochemical analysis is effectual (Xia et al, 1998). The main elements are tested by using the XRF method and the rare earth elements (REE for short) and trace elements (TE for short) with the ICP-MS in the Guiyang Institute of Geochemistry, CAS (Tables 1 and 2). There are six samples of early-stage rhyolite (No. Sm-1-1–6), four samples of early-stage basalt (No. Sm-3-1, 2, 3 and 6), which are interlayered in the rhyolite, in the lower part and six samples of late-stage basalt (No. Sm-2-1–6) in the upper part. The rhyolite contains SiO_2 ranging from 69% to 70%, Na_2O+K_2O from 5.46% to 8.00% and K_2O/Na_2O from 0.88 to 1.80, and falls on the rhyodacite field in the SiO_2-Zr/TiO_2 sorting diagram (Fig. 2) (Winchester et al., 1977), and on the subalkaline field in the SiO_2-(Na_2O+K_2O) diagram (Fig. 3) (Hyndman, 1985). Among the 10 basalt samples, four early ones (in the lower part and interlayered in rhyolite) have K_2O+Na_2O ranging from 4.95% to 8.81% and K_2O/Na_2O from 0.54 to 1.50, and fall on the shoshonite field in the K_2O-SiO_2 diagram (Qiu, 1985) and on the basanite and alkaline basalt fields in the SiO_2-Zr/TiO_2 diagram (Fig. 2). The late six basalt samples fall on the subalkaline basalt field in the SiO_2-Zr/TiO_2 diagram and their Na_2O/K_2O is between 5.11 and 7.89, showing strong Na-enrichment and characteristics of tholeiite. In the SiO_2–(K_2O+Na_2O) diagram, the early-stage basalt occurs in the alkaline field, while three of the late-stage basalt samples occur in the subalkaline field close to the boundary and the rest ones in the alkaline field. From early to late, the alkalinity declines gradually. Synthesized analysis of the chemical compositions of the basalts shows that the content of K decreases and that of Na increases gradually from early to late with increasing M/F and decreasing TiO_2 and MnO, indicating a trend from alkaline through calc-alkaline to tholeiite series (Fig. 4) (Mullen, 1983). All of the above shows that the volcanic rocks were formed in a constantly extending environment. The three early-stage shoshonite samples have high REE compositions, the ΣREE is between 243.30×10^{-6} and 505.18×10^{-6}, but the ΣREE of sample Sm-3-1 is similar to that of the late basalts, and δEu=0.81–0.69. These show

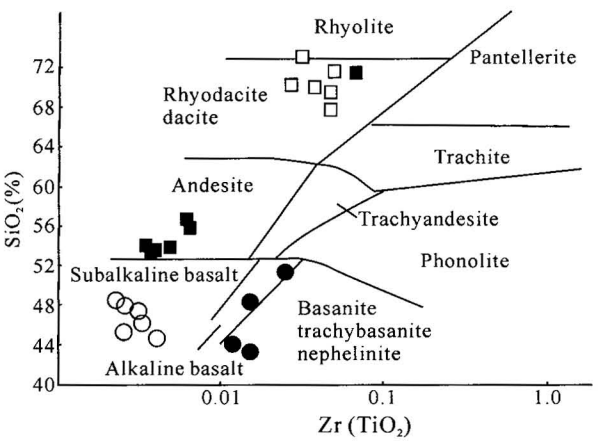

Fig. 2. SiO_2-Zr/TiO_2 sorting diagram of volcanic rocks. Solid circles represent the early-stage basalts from the AG (back-arc), blank circles represent the late-stage basalts from the AG, blank square represents the rhyolites from the AG and solid square represents the (basaltic) andesite from the TG (island arc).

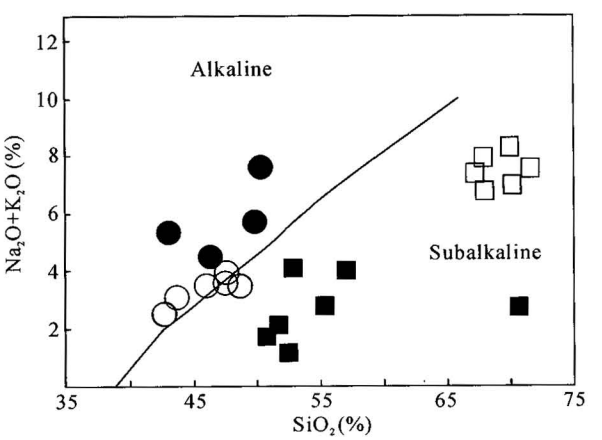

Fig. 3. SiO_2-(Na_2O+K_2O) diagram of volcanic rocks. Legends same as in Fig. 2.

that the basalts have small to medium Eu negative anomalies. $(La/Y)_N$=4.06–7.57 and LREE/HREE= 4.42–7.45 indicate that they are LREE enriched. All these are characteristic of intraplate basalt. For the late-stage basalts, one can see the following facts: the ΣREE ranges from 36.5 to 67.4×10^{-6}, close to that of ocean tholeiite; δEu=0.83–1.13; there is no evident Eu anomaly; $(Ce/Yb)_N$=1.52–2.48; and the LREE and HREE show certain differentiations. In the chondrite-normalized spider diagram, the late-stage basalts have slightly higher LREE compared with that of ocean tholeiite (Fig. 5). We thus deduce that the late-stage basalts came from the mantle and were slightly contaminated by continental crust. For the rhyolites, the following can be seen: the ΣREE ranges from 358.1×10^{-6} to 479.7×10^{-6}, δEu=0.65–0.69, there are moderate Eu negative anomalies, LREE/HREE=3.54–3.93, $(La/Y)_N$=7.86–10.51 and $(Ce/Yb)_N$=7.91–9.19, showing distinct LREE and HREE differentiations.

The REE spider diagram shows that the rhyolites from the AG are consistent to each other (Fig. 6). Comparing the REE spider diagram of the rhyolites with that of the basalts, one can see that the rhyolites might come from the same source as the early basalts, which are products of continental crust remelting. The late basalts are quite different from the early ones, and they might come from mantle partial melting. On the geological sections, the thickness of the rhyolite is four to six times that of the basalt, which prove that the basalt and the rhyolite could not be the products of mantle batch melting. As for the TE (Table 2), in the N-MORB-normalized spider diagram, the three early shoshonite samples show characteristics of the alkaline intraplate basalt (Fig. 7) (Pearce, 1983). The contents of Hf, Ti, Sm, Y, Yb and Sc (HFSE) of the late-stage basalts are similar to those of N-MORB, and the distribution patterns are also similar to those of tholeiitic-alkaline N-MORB. From early to late, Th/Yb declines gradually but Zr/Nb and Ba/Nb only have little changes. In the Th-Hf/3-Ta and Zr/4-Nb×2-Y triangle

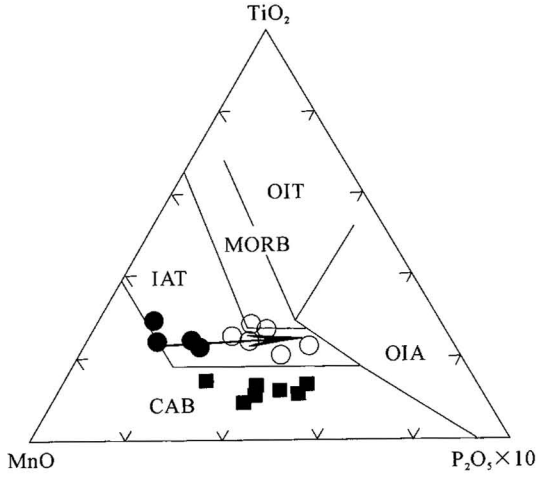

Fig. 4. TiO_2-MnO-P_2O_5×10 diagram of volcanic rocks from different tectonic backgrounds.
Legends same as in Fig. 2

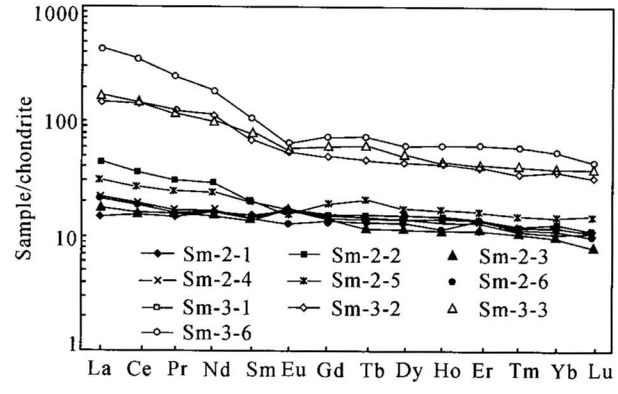

Fig. 5. REE chondrite-normalized spider diagram of the basalts from the AG.

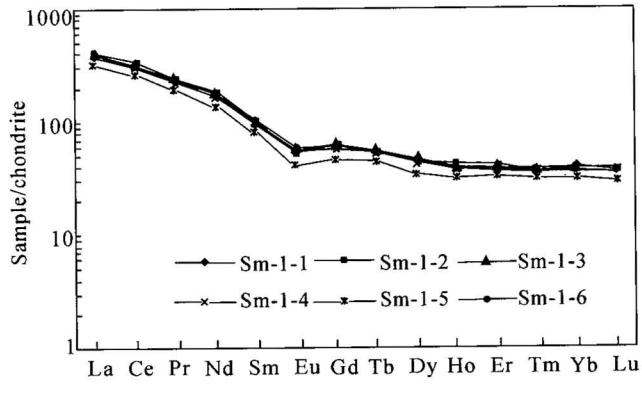

Fig. 6. REE chondrite-normalized spider diagram of the rhyolites from the AG.

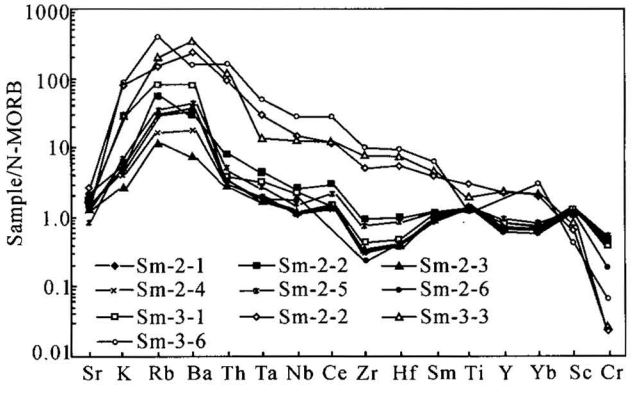

Fig. 7. N-MORB-normalized spider diagram for the TE of the basalts from the AG.

Table 1 REE composition of metamorphic volcanic rocks

Sample No.	Lithology	La	Ce	Pr	Nd	Sm	Eu	Gd	Tb	Dy	Ho	Er	Tm	Yb	Lu	ΣREE	δEu	$(La/Yb)_N$	LREE/HREE
Sm-1-1	Meta-rhyolite	90.17	191.30	21.17	78.78	14.63	3.14	12.78	2.12	11.72	2.31	6.56	0.97	6.72	0.90	505.17	0.68	9.62	7.44
Sm-1-2	Meta-rhyolite	98.41	207.90	22.89	86.89	15.76	3.28	13.63	2.13	12.16	2.31	6.90	0.96	6.39	0.89	443.31	0.67	11.03	9.05
Sm-1-3	Meta-rhyolite	92.13	197.79	22.06	81.25	14.74	3.04	12.12	1.95	10.92	2.16	5.80	0.92	5.99	0.84	480.55	0.67	11.02	9.58
Sm-1-4	Meta-rhyolite	88.12	188.85	20.32	75.92	14.19	3.04	11.74	1.95	10.66	2.11	6.11	0.86	5.70	0.80	451.77	0.70	11.08	10.09
Sm-1-5	Meta-rhyolite	73.64	157.15	17.11	62.70	12.08	2.42	9.54	1.61	8.59	1.76	5.37	0.80	5.24	0.74	430.42	0.66	10.06	9.77
Sm-1-6	Meta-rhyolite	97.81	206.21	22.84	84.36	15.11	3.00	12.52	2.03	11.01	2.28	6.50	0.92	6.40	0.88	358.82	0.64	10.96	9.65
Sm-2-1	Hornblende schist	3.61	9.62	1.39	6.99	2.43	0.76	2.88	0.52	3.30	0.67	1.97	0.27	1.74	0.28	36.47	0.88	1.48	2.13
Sm-2-2	Hornblende schist	10.62	22.62	2.95	13.24	3.11	0.99	3.53	0.63	3.85	0.79	2.22	0.34	2.52	0.36	67.80	0.91	3.01	3.75
Sm-2-3	Amphibolite	4.25	9.93	1.46	6.97	2.18	0.81	2.77	0.46	3.02	0.65	1.96	0.27	1.76	0.21	36.72	1.00	1.73	2.31
Sm-2-4	Amphibolite	5.06	11.56	1.56	7.98	2.52	1.05	3.14	0.60	3.69	0.74	2.30	0.32	2.05	0.29	42.91	1.13	1.77	2.26
Sm-2-5	Amphibolite	7.17	16.46	2.26	11.15	3.03	0.92	3.96	0.74	4.33	0.94	2.71	0.37	2.46	0.37	56.92	0.81	2.09	2.58
Sm-2-6	Amphibolite	1.66	11.41	1.60	7.57	2.22	0.76	2.67	0.51	3.34	0.65	1.88	0.29	1.91	0.26	39.78	0.95	0.61	2.45
Sm-3-1	Amphibolite	4.77	11.49	1.59	8.20	2.62	1.07	3.16	0.59	3.72	0.81	2.21	0.34	2.18	0.28	43.07	1.13	1.57	2.23
Sm-3-2	Amphibolite	35.57	89.28	11.71	52.79	10.67	3.17	10.36	1.75	10.85	2.34	6.75	0.90	6.28	0.83	243.30	0.91	4.05	5.07
Sm-3-3	hornblende schist	39.10	92.37	11.40	17.00	12.14	3.31	12.73	2.28	13.2	2.56	6.94	1.03	6.65	0.98	251.81	0.81	4.21	4.42
Sm-3-6	amphibolite	100.71	213.83	23.00	87.24	16.85	3.72	15.33	2.74	15.86	3.46	10.27	1.50	9.54	1.21	505.18	0.69	7.57	7.45
1028-I1	meta-basalt	1.40	3.41	0.44	1.87	0.54	0.24	0.80	0.14	1.02	0.25	0.74	0.10	0.85	6.07	0.15	1.13	1.17	0.78
1028-I2	meta-andesite	0.95	2.65	0.32	1.78	0.50	0.18	0.74	0.16	1.11	0.29	0.81	0.14	0.98	7.20	0.16	0.91	0.69	0.55
1028-I3	meta-rhyolite	7.32	17.15	2.14	9.73	2.52	0.52	2.82	0.48	2.97	0.67	2.16	0.32	2.46	18.47	0.40	0.60	2.12	1.20
1028-I4	meta-basalt	1.06	2.84	0.34	1.64	0.54	0.21	0.70	0.17	1.05	0.23	0.72	0.13	0.80	5.807	0.16	1.08	0.94	0.63
1028-I5	meta-andesite	1.57	3.56	0.43	2.00	0.61	0.20	0.73	0.15	0.88	0.20	0.75	0.11	0.84	5.825	0.13	0.94	1.32	0.845
1028-I6	meta-nbasalt	1.35	3.23	0.42	1.96	0.53	0.24	0.81	0.14	1.04	0.23	0.70	0.10	0.76	5.97	0.15	1.13	1.26	0.79
1028-I7	meta-andesite	1.17	3.06	0.37	1.70	0.48	0.16	0.65	0.13	0.92	0.19	0.68	0.10	0.79	5.06	0.12	0.87	1.06	0.75

Notes: The samples are tested by using ICP-MS in the Guiyang Institute of Geochemistry, CAS, in $\times 10^{-6}$.

Table 2 Trace elements composition of the metamorphic volcanic rocks

Sample No.	Lithology	Sr	K	Rb	Ba	Th	Ta	Nb	Ce	Zr	Hf	Sm	Ti	Y	Yb	Sc	Cr	Th/Yb	Nb/Ta
Sm-2-1	Hornblende schist	117.66	0.46	17.94	230.03	0.35	0.22	3.84	9.62	24.14	0.82	2.43	0.95	18.433	1.748	48.20	143.05	0.199	17.07
Sm-2-2	Hornblende schist	80.36	0.36	33.31	177.86	1.00	0.57	9.23	22.62	69.37	2.00	3.11	1.27	20.07	2.52	46.51	119.49	0.396	15.95
Sm-2-3	Amphibolite	113.24	0.16	6.38	46.86	0.31	0.22	3.74	9.93	19.61	0.85	2.18	0.88	19.02	1.76	43.38	127.3	0.176	16.85
Sm-2-4	Amphibolite	134.41	0.24	9.51	112.76	0.35	0.26	3.84	11.56	51.33	1.48	2.52	1.00	21.40	2.04	47.91	136.04	0.174	14.78
Sm-2-5	Amphibolite	77.46	0.41	19.60	266.91	0.62	0.37	5.52	16.46	56.19	1.71	3.03	1.02	26.73	2.46	46.75	51.70	0.253	14.73
Sm2-6	Amphibolite	192.93	0.32	16.57	231.24	0.41	0.24	6.54	11.41	23.18	0.86	2.22	0.88	17.61	1.91	44.08	48.02	0.215	26.82
Sm-3-1	Amphibolite	156.49	1.78	43.91	503.80	0.44	0.43	8.20	11.49	32.04	1.00	2.62	0.96	22.38	2.18	48.32	105.45	0.203	19.07
Sm-3-2	Amphibolite	239.53	4.74	82.45	1464.55	11.34	3.86	52.79	89.23	377.25	11.03	10.67	2.17	64.11	6.28	25.35	6.18	1.803	13.68
Sm-3-3	Hornblende schist	176.74	1.69	115.72	2081.01	14.80	1.85	47.00	92.37	581.43	15.52	12.14	1.44	65.29	6.64	31.61	7.21	2.227	25.31
Sm-3-6	Amphibolite	114.01	5.32	218.44	957.91	19.30	6.63	102.52	213.83	748.25	19.46	16.85	0.91	96.18	9.54	16.52	18.69	2.024	15.46
1028-I1	Meta-basalt	191.29	0.82	26.17	161.12	0.34	0.04	0.37	3.41	9.84	0.40	0.54	0.13	6. 07	0.85	43.83	91.47	0.39	8.78
1028-I2	Meta-andesite	191.68	0.79	14.77	112.55	0.45	0.04	0.43	2.65	12.53	0.49	0.50	0.14	7.20	0.98	45.25	34.73	0.45	10.65
1028-I3	Meta-rhyolite	140.38	0.41	17.55	82.96	1.48	0.25	3.89	17.15	80.55	2.28	2.52	0.15	18.47	2.46	17.66	7.36	0.60	15.65
1028-I4	Meta-basalt	177.61	0.49	19.26	79.19	0.35	0.04	0.57	2.84	13.08	0.51	0.54	0.14	5.80	0.80	49.80	29.34	0.43	15.62
1028-I5	Meta-andesite	181.79	0.72	16.71	121.15	0.42	0.04	0.39	3.56	10.99	0.37	0.61	0.12	5.82	0.84	41.81	52.82	0.49	10.10
1028-I6	Meta-nbasalt	189.71	0.53	24.97	147.22	0.26	0.03	0.33	3.23	8.57	0.42	0.53	0.12	5.97	0.76	42.54	64.37	0.34	10.77
1028-I7	Meta-andesite	173.97	0.33	25.62	122.96	0.35	0.05	0.62	3.06	13.58	0.51	0.48	0.15	5.06	0.79	48.62	31.01	0.44	11.98

Notes: The samples are tested by using ICP-MS in the Guiyang Institute of Geochemistry, CAS, in $\times 10^{-6}$ except for K and Ti which are in $\times 10^{-2}$ (tested with the XRF method)

diagrams (Figs. 8 and 9) (Wood, 1979), the late-stage basalts occur in the P-MORB field. In the Th-Hf/3-Nb/16 diagram (not shown in the paper), the early-stage shoshonites occur in the intraplate basalt field, while the late-stage basalts in the P-MORB and N-MORB fields. In view of the geochemistry of the volcanic rocks of the AG, the rocks are thought to be formed in a pull-apart environment.

3 Geochemistry of Island-Arc Volcanic Rocks

This volcanic sequence refers to a suite of low-grade metamorphic but strongly-deformed TG andesite and basaltic andesite intercalated with minor rhyolite and marble. They occurs to the south of Minfeng and Yutian. Low-mature clasolite can be seen in some places. Its outcropping thickness reaches several thousand meters. Geochemical composition (for seven samples, No. 1028-11–17: six are andesite and only 1028-13 is rhyodacite) shows that the SiO_2 content of the (basaltic) andesite ranges from 52.36% to 58.30%, averaging 54.55%; and that the TiO_2 content is low (<0.3%), averaging 0.22%. Na_2O+K_2O=1.70%–3.57%, Na_2O/K_2O= 2.44–4.61, M/F=0.62–0.78, and MgO/(MgO+TFe)= 0.36–0.45. In the SiO_2-Zr/TiO_2 sorting diagram, they occur in the andesite field but are very close to the subalkaline basalt field (Fig. 2). In the SiO_2–(Na_2O+K_2O) diagram, they fall in the subalkaline field (Fig. 3) and in the TiO_2-MnO_2-P_2O_5×10 diagram in the calc-alkaline field (Fig. 4). It is thus concluded that the volcanic rocks from the TG are calc-alkaline. The andesites have very low

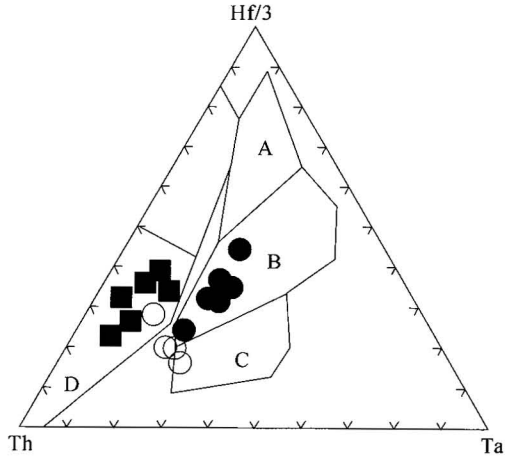

Fig. 8. Th-Hf/3-Ta diagram of the basalts from different tectonic environments.
Legends same as in Fig. 2; A – N-MORB; B – P-MORB; C – WPB; D – IAT.

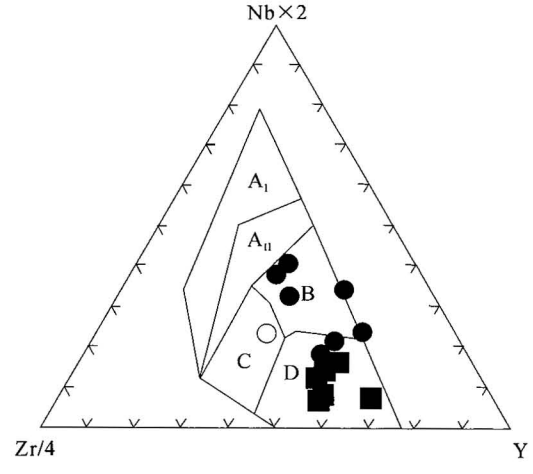

Fig. 9. Zr/4–Nb×2–Y diagram of the basalts from different tectonic environments.
Legends same as in Fig. 2; A – N-MORB; B – P-MORB; C – WPB; D – IAT.

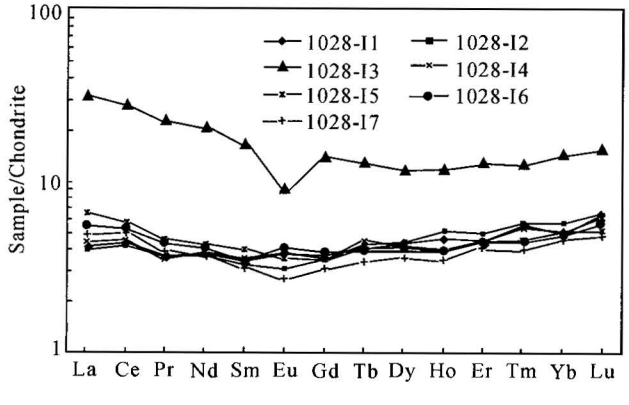

Fig. 10. REE chondrite-normalized spider diagram of the (basaltic) andesites from the TG.

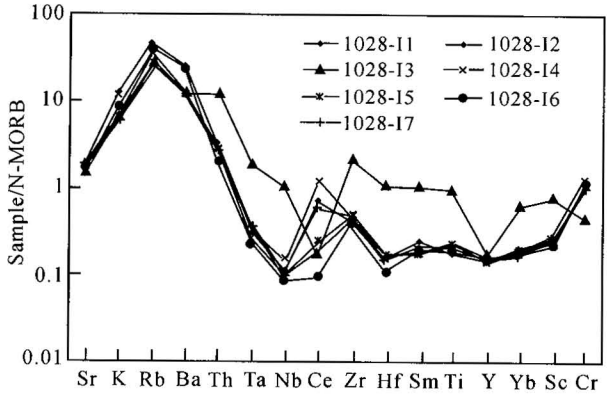

Fig. 11. N-MORB-normalized spider diagram for the TE of the (basaltic) andesites from the TG.

ΣREE which ranges from 15.52×10^{-6} to 17.92×10^{-6}, similar to that of ocean tholeiite and different from that of the volcanic rocks occurring on the continental margin arc that is enriched in LREE. We deduce that the andesites came from mantle (Yogodzinski et al., 1998). Their $(La/Yb)_N$=0.69–1.33 and $(Ce/Yb)_N$=0.75–1.17, which indicate that the LREE and HREE have no obvious differentiations. δEu=0.87–1.13 and there are very weak Eu anomalies. The REE chondrite-normalized spider diagram shows that the REE distribution pattern is similar to that of ocean tholeiite (Fig. 10), and that the andesites came from depleted mantle with no contamination of continental crust. As for the TE, Th/Yb=0.04–0.10, Th/Ta=5.92–11.22, Zr/Hf=20.46–29.40, and Ti/V= 4.33–5.10. In the N-MORB-normalized diagram (Fig. 11), LILE such as Rb, Ba, Th and K are enriched and HFSE depleted, thus yielding high Th/Ta, Ce/Yb and La/Nb ratios. All these show the characteristics of island-arc volcanic rocks (Pearce, 1983). Although a Ce acme occurs in the TE spider diagram, the Th and Ce values are close to those of N-MORB, which indicates almost no contamination of the subduction zone (Zhang et al., 1995). In the Th-Hf/3-Ta and Zr/4–Nb×2–Y triangle diagrams (Figs. 8 and 9), all samples fall in the field of island arc.

To sum up, the TG vocanites to the south of Minfeng and Yutian consist main of calc-alkaline (basaltic) andesites intercalated with minor calc-alkaline rhyolite. The rock association shows the characteristics of island-arc volcanlites. The REE and TE indicate that the rocks came from depleted mantle with no contamination of the subduction zone. We deduce that the magma is the product of the interaction of the subduction ocean crust and mantle (Matthew et al., 1999).

4 Ages of Volcanic rocks

In our field work we observed the Silu Group of the Qingbaikou'an System (1000–800 Ma) angular-unconformably overlying the AG (Ma, 1989) along the Buqiong and Xinjiang-Tibet Roads. Either deformation intensity or metamorphism of the AG is lower than those of the Archean–Paleoproterozoic Heluositan and Karakax Groups, so the age of the volcanic rocks is limited to Mesoproterozoic. Nd isotope analysis of the six late-stage basalt samples from the AG (tested by Qiao Guangsheng, Institute of Geology and Geophysics, CAS) indicates that the single-phase T_{DM} of the rocks ranges from 1500 to 1900 Ma, and that the isochron age is 1200±63 Ma. Considering that the formation age of the rocks cannot be older than its model age and that the Neoproterozoic overlies the volcanic rocks angular-unconformably, the isochron age is considered to be the formation age. The ^{40}Ar-^{39}Ar plateau ages of hornblende from amphibolite and biotite in metarhyolite from the AG are 1050±0.93 Ma and 1021±1.08 Ma respectively (Fig. 12), so 1050 Ma should be the closing time of the volcanic-sedimentary basin and the time of metamorphism of the volcanic rocks. As for the island-arc volcanic rocks of the TG, predecessors though that they belong to the Jixianian Period, but no isotope data are available. The Nd content of the rocks is too low for this analysis to get good results. Our field work reveals that Sinian tillite, which can be correlated with the Sinian System on the AG, directly lay upon TG around Ao'yiqieke unconformably. In the ridge area of the Western Kunlun Mountains, the Alamasi Group of the Jixianian Period, which lines in the same tectonic belt with the TG, unconformably overlies the Sailajiazitage Group of the Changcheng Period (1800–1400 Ma), so the TG should belong to the Jixianian Period. We believe that the island-arc and the back-arc basin volcanic rocks discussed above are coeval products of different tectonic settings.

5 Conclusions

Based on petrostratigraphic and geochemical characteristics of the Mesoproterozoic volcaniltes of the Western Kunlun Mountains, the authors hold that the rock

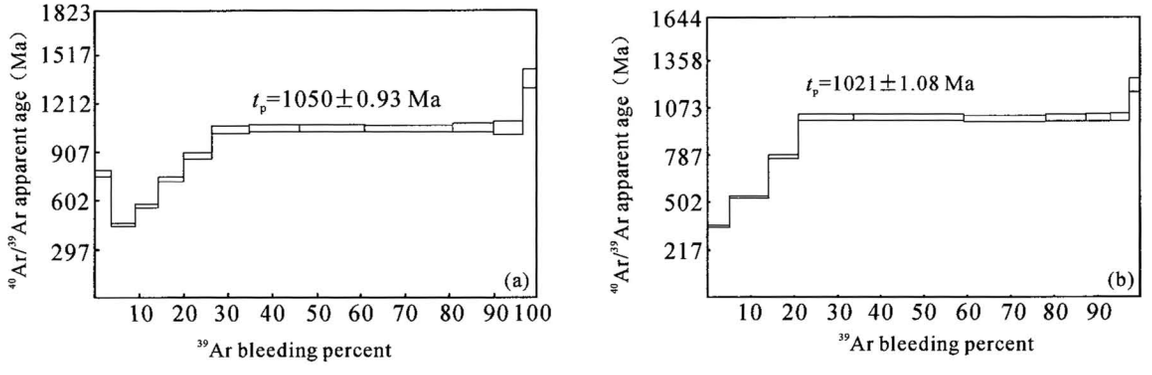

Fig. 12. ^{40}Ar-^{39}Ar plateau ages of metamorphic minerals in the AG: hornblende (a) and biotite (b).

associations of the AG were formed in a back-arc rifting setting; while the TG volcanic sequence, in an island arc setting. In view of their space distribution, the island-arc volcanic sequence occurs in the south belt and the back-arc basin volcanic sequence in the north. Although the two sequences are not connected with each other laterally, they actually represent volcanic-sedimentary rock associations of different tectonic settings of Mesoproterozoic island arc and back arc. We consider that the island-arc volcanic rocks in the western part were concealed during the late tectonic evolution and the volcanic-sedimentary sequence in the eastern part, which represents a back-arc setting, was covered by the Quaternary formations.

Jiang et al. (1992, 2000) pointed out that the basements of the south and north sides of the central orogen have different characters: the north is a hard or North China-type basement, while the south is a soft or the Yangtze-type basement. Earlier studies have revealed that the ancient Chinese land formed at the late Paleoproterozoic (Ren et al., 1999) began to rift in the Mesoproterozoic (1800 Ma), and that the Qiangtang block was separated from the Tarim plate to form the Kangxiwar ocean in-between (Jiang et al., 2000) (Fig. 13A, B). The Kangxiwar oceanic crust began to underthrust towards the ancient Tarim plate during the Jixianian Period, and the unconformity between the Jixian and Changcheng strata maybe indicate the transition from extension to convergence. In this period, no magmatic activity occurred in the south of the Kangxiwar area, which indicates that the subduction took place from south to north. This subduction brought about an island arc on the south margin of the ancient Tarim plate to give rise to back-arc rifting (Fig. 13C, D), thus forming a back-arc basin. The tholeiite is developed in the upper part of the AG, showing that the back-arc basin has an environment of a small ocean basin (Fig. 13D). After the close of the Kangxiwar Ocean, a powerful convergence momentum drove the back-arc oceanic crust to subduct from north to south towards the island arc (Fig. 13E). Because the unmetamorphosed Neoproterozoic strata overlie the AG unconformably and the peak metamorphism of the AG took place at ca. 1.05 Ga, the folding and orogeny of the back-arc basin and the consumption of the Mesoproterozoic sedimentary basin should occur at the end of the Mesoproterozoic (Fig. 13F).

The ascertainment of the Jixianian island arc and back-arc volcanic-sedimentary sequence in West Kunlun, and the timing of the orogeny and metamorphism of the volcanic-sedimentary basin indicate that there existed a Grenville orogenic event in the north of the Qinghai-Tibet plateau (Lu, 1998), which is 200 Ma earlier than the Tarim movement in the Xinjiang and Jinning movement in north of Yangtze block (Zhang et al, 2000). This study has thus provided important geological evidence for finding out the location of the ancient Tarim plate in the Rodinia supercontinent.

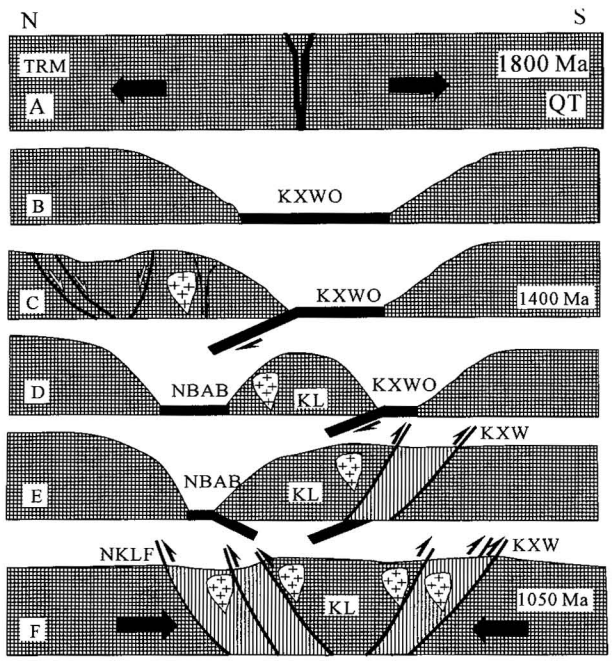

Fig. 13. A tectonic evolution model for the Western Kunlun Mountains in the Mesoproterozoic.
TRM – ancient Tarim plate; QT – Qiangtang block; KXWO – Kangxiwar Ocean;NBAB – North Kunlun back-arc basin; KL – Kunlun block; KXWF – Kangxiwar fault; NKLF – North Kunlun fault.

Acknowledgements

This work was supported by the Project of "Precambrian geological issues in China" (No. 200113900070). Sincere thanks are due to the reviewers for their hard work in reviewing and correcting the manuscript.

Manuscript received Nov. 20, 2001
accepted July 10, 2002
edited by Hao Ziguo and Liu Xinzhu

References

Xinjiang Bureau of Geology and Mineral Resources, 1993. *Regional Geology of Xinjiang Uygur Autonomous Region.* Beijing: Geological Publishing House, 22–31(in Chinese with English abstract).

Guo Kunyi, Wang Aiguo and Zhang Chuanlin, 2002. Lithology of the Ailiankate Group in eastern part of the Western Kunlun orogen and its tectonic significance. In: *80th Anniversary of*

the Geological Society of China. Beijing: Geological Publishing House, 105–110 (in Chinese with English abstract).

Hyndman, D. W., 1985. *Petrology of Igneous and Metamorphic Rocks*. New York: McGraw-Hill, 135–141.

Winchester, J. A., and Floyd, P. A., 1977. Geochemical discrimination of different magma series and their differentiation products using immobile elements. *Chemical Geology*, 20(3): 325–343.

Jiang Chunfa, Yang Jingsui and Feng Binggui, 1992. *Opening and Closing Tectonics of Kunlun*. Beijing: Geological Publishing House, 12–38 (in Chinese with English abstract).

Jiang Chunfa, Wang Zongqi and Li Jinyi, 2000. *Opening and Closing Tectonics of the Central Orogen*. Beijing: Geological Publishing House, 73–103 (in Chinese with English abstract).

Liu Dequan, Tang Yanling and Zhou Ruhong, 1998. Five-Stage Moldel of the Palaeozoic Crustal Evolution in Xinjiang. *Acta Geologica Sinica (English edition)*, 72(4): 339–349.

Lu Sŏngnian, 1998. A review of advance in the research on the Neoproterozoic Rodinia Supercontinent. *Geological Review*, 44(5): 489–495 (in Chinese with English abstract).

Ma Shipeng, Wang Yuzhen and Fang Xilian, 1989. The Sinian at north slope of the Western Kunlun Mountains. *Xinjiang Geology*, 7(4): 67–79 (in Chinese with English abstract).

Matthew, I.L., Nancy, V.W., and Lorne, D.A., 1999. Partial melting of a refractory subducted slab in a Paleoproterozoic island arc: Implication for global chemical cycles. *Geology*, 27(8), 731–734.

McDonough, W.F., 1991. Partial melting of subducted oceanic crust and isolation of its residual eclogitic lithology. *Royal Society of London Philosophical Transactions*, ser. A,. 335: 407–418.

Miao Changquan, 1993. *Precambrian system and stromatolites in the Kunlun Mountains and Altun Mountains, Xinjiang*. Urumqi: Xinjiang Science, Technology and Hygiene Publishing House, 47–96 (in Chinese with English abstract).

Mullen, E.D., 1983. $MnO/TiO_2/P_2O_5$: A minor element discrimination for basaltic rocks of oceanic environments and its implications for petrogenesis. *Earth Planet. Sci. Lett.*, 62: 53–62.

Pearce, J.A, 1983. The role of sub-continental lithosphere in magma genesis at destructive plate margins. In: Hawkesworth et al. (eds.), *Continental Basalts and Mantle Xenolith*. Nantwich: Shiva, 230–249.

Qiu Jiaxiang, 1985. *Magmatite Petrology*. Beijing: Geological Publishing House, 207–209 (in Chinese).

Pan Yusheng, Wang Yi, Matte, Ph., and Tapponnier, P., 1995. Geology Along the Line From Yecheng to Shiquanhe and Tectonic Evolution of the Region Involved. *Acta Geologica Sinica (English edition)*, 8(2): 119–134.

Ren Jishun, Wang Zuoxun, Chen Bingwei and Jiang Chunfa, 1999. *Chinese Tectonic Structure, a View from the Whole Globe*. Beijing: Geological Publishing House, 7–9 (in Chinese).

Wang Yuzhen, 1983. Age and tectonic significance of Yishake Group in Western Kunlun. *Xinjiang Geology*, 1(1): 1–8 (in Chinese with English abstract).

Wood, D.A., 1979. A variably veined suboceanic upper mantle–genetic significance for mid-ocean ridge basalts from geochemical evidence. *Geology*, 7: 499–503.

Xia Linqi, Xia Zuchun and Xu Xueyi, 1998. Early Palaeozoic mid-ocean ridge-ocean island and back-arc volcanism in the North Qilian Mountains. *Acta Geologica Sinica* (Chinese edition), 72(4): 301–312 (in Chinese with English abstract).

Xiao Xuchang and Li Tingdong, 1998. Lithosphere structure, uplifting system and its influence on the continental deformation of Qinghai-Tibet Plateau. *Geological Review*, 44(1): 111 (in Chinese with English abstract).

Yogodzinski, G.M., and Kelemen, P.B., 1998. Slab melting in the Aleutians: Implications of an ion probe study of clinopyroxene in primitive adakite and basalt. *Earth Planet. Sci. Lett.*, 158: 53–65.

Zhang Qi, Zhang Zongqing and Sun Yong, 1995. Trace element and isotope geochemistry of the metamorphic basalt in Danfeng Group in Shanxian-Danfeng, Shaanxi. *Acta Petrologica Sinica*, 11(1): 43–54.

Zhang Chuanlin, Dong Yongguan and Yang Zhihua, 2000. Two ophiolit belts in the Qinling orogen and their constraints on the tectonic evolution of the Qinling-Dabie Orogen. *Acta Geologica Sinica* (Chinese edition), 74(4), 313–324 (in Chinese with English abstract).